Aerospace Science and Technology 175 (2026) 112056

Contents lists available at ScienceDirect

Aerospace Science and Technology

journal homepage: www.elsevier.com/locate/aescte

Kinetic and experimental study of Mn(III) acetylacetonate for green hypergolic ignition in HTP/Kerosene systems

Prakhar Jindal *, Jyoti Botchu

Space System Engineering Section, Space Engineering, Faculty of Aerospace Engineering, TU Delft. Kluyverweg 1 2629 HS Delft, Netherlands

ARTICLE INFO

Editor: Cummings Russell

Keywords:
Mn(III)AA
Hypergolic ignition
Hydrogen peroxide
Green propellants
Ignition delay time
Arrhenius parameters

ABSTRACT

The transition towards non-toxic, high-performance spacecraft propulsion has positioned highly concentrated hydrogen peroxide (HTP) and kerosene as a leading green propellant combination. However, achieving reliable hypergolic ignition in non-polar hydrocarbons remains a critical challenge due to significant physical mixing limitations and high chemical activation barriers. This study investigates the catalytic efficacy of Manganese(III) acetylacetonate (Mn(III)AA) dissolved in aviation-grade kerosene to enable rapid hypergolicity with 98% HTP. High-speed imaging and thermal diagnostics were employed to map the ignition delay time (IDT) across a range of catalyst loadings (0.5–10 wt%) and oxidizer-to-fuel ratios (4.5–7.5). The results demonstrate that Mn(III)AA is highly effective, achieving a minimum IDT of 25 ms at 50°C. Kinetic analysis revealed a significant reduction in apparent activation energy (9 to 14 kJ/mol), accelerating the chemical reaction rate until the system becomes limited by physical mixing processes. Notably, a non-linear performance trend was observed, where catalyst additions beyond 5 wt% yielded diminishing returns, suggesting a saturation threshold for practical engine design. These findings establish Mn(III)AA as a viable, high-efficiency additive for green bipropellant systems.

1. Introduction

The global aerospace industry is increasingly focused on developing sustainable and environmentally benign propulsion systems to replace traditional, highly toxic hypergolic propellants such as monomethylhydrazine (MMH) and mixed oxides of nitrogen (NTO) [1,2]. This drive is significantly reinforced by stringent regulatory frameworks, such as the European Union's REACH (Registration, Evaluation, Authorisation and Restriction of Chemicals) program [3], which increasingly restricts the use of hazardous substances including hydrazines. These conventional propellants, while offering reliable ignition without external sources, pose significant environmental hazards, health risks during handling, and incur substantial costs for storage, transportation, and disposal [4–6]. That has driven a global shift towards "greener" alternatives that maintain performance while mitigating these drawbacks.

High-Test Peroxide (HTP), a highly concentrated solution of hydrogen peroxide, has emerged as a promising green oxidizer due to its high oxygen content, non-toxic decomposition products (water and oxygen), and high density [7,8]. When paired with hydrocarbon fuels like kerosene, HTP can form hypergolic bipropellant systems, offering the critical advantage of self-igniting capabilities without the need for complex external ignition sources or conventional catalyst beds [9,10]. This inherent hypergolicity, facilitated by an appropriate catalyst, simplifies engine design, reduces system mass, enhances operational safety, and contributes significantly to the overall sustainability and cost-effectiveness of space missions [11].

Despite these advantages, achieving reliable and consistently short ignition delay times (IDTs) with HTP/hydrocarbon systems often requires effective catalytic additives [12,13]. Metal-organic complexes, particularly those involving manganese, have shown considerable promise due to their ability to accelerate HTP decomposition and facilitate subsequent fuel oxidation [12,13]. While various catalysts have been explored, a comprehensive understanding of the kinetic and performance characteristics of specific novel catalysts, such as Mn(III) acetylacetonate (Mn(III)AA), across a wide range of operating conditions, remains crucial for their practical implementation and optimization in propulsion systems. Key ignition challenges include achieving short, consistent IDTs and complete combustion, ensuring operational safety and stability [14–17]. These are governed by complex interactions between physical and chemical delays, particularly droplet atomization and vaporization dynamics [18].

* Corresponding author.
E-mail addresses: p.jindal@tudelft.nl, prakharjindal@gmail.com (P. Jindal).

https://doi.org/10.1016/j.ast.2026.112056
Received 11 August 2025; Received in revised form 16 January 2026; Accepted 2 March 2026
Available online 3 March 2026

While various manganese-based catalysts have been explored in the literature, previous studies have predominantly focused on ethanol gels [12,13] or ionic liquids [9,10] as fuels. These solvent-rich systems present fundamentally different miscibility and ignition characteristics compared to pure hydrocarbons. To date, a comprehensive mapping of the kinetic and performance characteristics of Mn(III) acetylacetonate dissolved directly in aviation-grade kerosene has not been reported. To address this gap, this study aims to systematically investigate the performance, kinetic behavior, and practical implications of Mn(III)AA as a hypergolic catalyst in HTP/kerosene bipropellant systems. Through extensive open-air drop tests across varying HTP concentrations, catalyst loadings, oxidizer-to-fuel (O/F) ratios, and initial temperatures, IDTs are quantified, post-ignition flame characteristics are analyzed, and the multi-phase ignition process is explored. Furthermore, apparent kinetic parameters (activation energy and pre-exponential factor) are derived to interpret the underlying reaction mechanisms and identify optimal operating regimes. The insights gained from this research are expected to significantly contribute to the development of more efficient, reliable, and environmentally sustainable propulsion technologies for future space applications.

The remainder of this paper is organized as follows: Section 2 details the materials, experimental setup, and diagnostic methodologies employed. Section 3 presents the experimental results, including ignition delay measurements, kinetic parameter derivation, and flame temperature analysis, followed by a discussion on the physical-chemical coupling mechanisms. Finally, Section 4 summarizes the key conclusions and discusses the implications for future green propulsion technologies.

2. Materials and methods

2.1. Materials

Hydrogen peroxide (HTP) (70% (w/w), CAS No. 7722-84-1) and aviation-grade kerosene ($C_{15}H_{32}$, CAS No. 8008-20-6) were used as the oxidizer and fuel, respectively. Mn(III) acetylacetonate ((Mn(III)AA) Mn $(C_5H_7O_2)_3$, 99% pure, CAS No. 14024-58-9) served as the catalyst. All materials, purchased from Chemwatch, were of high purity and used as received. Table 1 details the physicochemical properties of the 98% HTP and Aviation-grade Kerosene. Further details on material specifications and preparation are provided in the Supplementary Information (Section S1).

2.2. Experimental setup and conditions

IDTs were measured using a standardized open-air drop test apparatus. The catalyzed fuel mixtures were prepared by dissolving Mn(III)AA directly into aviation-grade kerosene via vigorous magnetic stirring for 26–32 hours at 30°C to ensure homogeneity. Prior to testing, the fuel samples were thermostatted to the target initial temperatures (20°C or 50°C) to ensure thermal equilibrium at the moment of contact.

For each test, a fixed volume of 0.27 mL (270 μL) of HTP was dispensed using a precision syringe pump through an 18-gauge stainless steel blunt needle (1.2 mm O.D.) positioned at a fixed height of 10 cm onto a quiescent fuel pool. The fuel was contained in a chemically inert porcelain crucible to eliminate background catalytic effects. Between trials, the crucible was cleaned with acetone and ethanol, then oven-dried to ensure a pristine impact surface. The fuel volume was adjusted (0.061–0.102 mL) to achieve the target oxidizer-to-fuel (O/F) mass ratios.

Table 1
Physicochemical properties of the propellants used in this study (at 20°C).

Property	98% HTP	Aviation Kerosene (Jet A-1)
Density (g cm^{-3})	1.43	0.80
Viscosity (mPa·s)	1.25	1.64
Lower Heating Value (MJ kg^{-1})	2.8 (Decomp.)	43.2
Purity / Grade	98% (Rocket Grade)	Commercial Aviation Grade
Preparation	Vacuum Dehydration	Used as received (unfiltered)

The parametric space explored included HTP concentrations (85-98% w/w), Mn(III)AA catalyst loadings (0.5-10% w/w in fuel), O/F ratios (4.5, 5.5, 6.5, 7.5), and two initial temperatures (20°C and 50°C). A detailed schematic of the experimental setup and comprehensive experimental specifics are provided in the Supplementary Information (Section S2). It is noted that while these tests were conducted at ambient pressure, literature suggests IDTs for such systems typically reduce by 20-30% in pressurized environments, indicating enhanced performance in operational propulsion systems [12–20].

2.3. Data acquisition and analysis

IDTs were determined from high-speed camera footage captured at 6400 fps using a Photron FASTCAM NOVA S6, measuring the interval from droplet contact to first light emission. Post-ignition flame temperatures were recorded using a FLIR A655sc thermal imaging camera (spectral range 7.5–14.0 μm). To ensure a rigorous quantitative definition of ignition, a dual-validation approach was employed. The onset of visible light emission in the high-speed footage was cross-referenced frame-by-frame against synchronized thermal imaging data. Ignition was defined as the specific time-step where the appearance of a visible flame kernel coincided with a rapid, distinct temperature escalation ($dT/dt \gg 0$). For signal-to-noise handling, experiments were conducted under controlled, constant laboratory lighting to eliminate variable background reflections. The high temporal resolution (0.15 ms/frame) allowed for the clear differentiation between static ambient light and the dynamic, rapidly expanding wavefront of the ignition kernel, ensuring that the recorded IDT values represented genuine chemiluminescence.

To quantify the relative contributions of physical mixing versus chemical kinetics, the total IDT was deconvoluted into distinct mechanistic phases through frame-by-frame analysis. These phases were defined by specific visual criteria: (1) Decomposition Delay (t_{decomp}): the interval from droplet contact to the onset of visible white fume release, indicating rapid catalytic HTP decomposition; (2) Physical Delay (t_{phys}): the duration from fume onset to the formation of a distinct vapor plume or rapid volume expansion; and (3) Chemical Delay (t_{chem}): the time from vapor cloud formation to the first observable light emission. Quantitative uncertainty analysis was applied to this segmentation process; while the fundamental temporal resolution is 0.16 ms per frame, a conservative expanded uncertainty of ±3 frames (≈ ±0.5 ms) was assigned to each phase boundary to account for transitional visual gradients. Additionally, the apparent activation energy (E_a) and pre-exponential factor (A) were calculated using a two-point Arrhenius method based on IDT data collected at 20°C and 50°C. A minimum of 5 replicate tests were performed for each condition to ensure data reliability and reproducibility.

To account for the optical properties of the sooting hydrocarbon/HTP diffusion flame, radiometric corrections were applied using a constant emissivity (ϵ) of 0.90. It is acknowledged that spectral emissivity in turbulent flames can fluctuate (typically 0.85–0.95), introducing a measurement uncertainty of approximately ±20°C. Consequently, the temperature data reported herein are presented as indicative peak temperatures, serving primarily to compare the relative thermal intensity between different catalyst loadings rather than representing precise thermodynamic equilibrium temperatures.

3. Results and discussion

3.1. Overview of Mn(III)AA performance and ignition envelope

The experimental investigation demonstrates that Mn(III)AA effectively catalyzes the hypergolic ignition of HTP/kerosene bipropellant systems across a broad range of operating conditions. The shortest IDT observed at an initial temperature of 20°C was 40 ms, achieved with an O/F ratio of 7.5, 10 wt% catalyst loading, and 98% HTP concentration. Remarkably, elevating the initial temperature to 50°C further reduced the minimum IDT to 25 ms under the same optimal conditions. The minimum IDT of 25 ms achieved here is significantly lower than the 100+ ms delays often reported for non-catalyzed kerosene systems and is competitive with the 10–50 ms range observed in complex ethanol-gel systems [12–20], confirming the high efficiency of the Mn(III)AA complex in liquid hydrocarbons. This significant reduction at 50°C is primarily attributed to the enhanced thermal decomposition of HTP and improved fuel vaporization kinetics, both contributing to a faster overall reaction initiation. These low IDTs demonstrate Mn(III)AA's capability to facilitate rapid and reliable ignition, which is crucial for responsive propulsion systems.

Analysis of the comprehensive dataset, available in detail in the Supplementary Information (Section S4.1), which includes over 586 test points covering varied HTP concentrations, catalyst loadings, and O/F ratios, reveals distinct ignition envelopes for Mn(III)AA at both 20°C and 50°C. The ignition envelope, determined empirically from observed ignition thresholds, defines the specific range of HTP concentrations, catalyst loadings, and O/F ratios under which reliable spontaneous ignition occurs. At 20°C, ignition reliability is strongly dependent on higher HTP concentrations and catalyst loadings, particularly at lower O/F ratios. For instance, at O/F 4.5, ignition was not observed for HTP concentrations below 95% at 0.5 wt% catalyst, and below 93% at 1 wt% catalyst. Similarly, at O/F 5.5, HTP concentrations below 93% resulted in no ignition at 0.5 wt% catalyst, and below 90% at 1 wt% catalyst. This overall behaviour is visually represented in Fig. 1.

These "no ignition" zones delineate the boundaries of the ignition envelope at lower temperatures. As HTP concentration and catalyst loading increase, the ignition envelope expands, leading to more consistent and shorter IDTs across the tested conditions. The improved performance at higher HTP concentrations can be attributed to the increased availability of reactive oxygen species upon HTP decomposition, which drives the subsequent fuel oxidation more vigorously [21, 22]. Similarly, higher catalyst loadings provide more active sites, accelerating the initial decomposition of HTP and thus shortening the overall ignition process. The robustness of Mn(III)AA to initiate hypergolic reactions even at moderate catalyst loadings and HTP concentrations highlights its potential for practical applications where minimizing catalyst content and operating with slightly lower HTP grades might be desirable for cost or safety considerations.

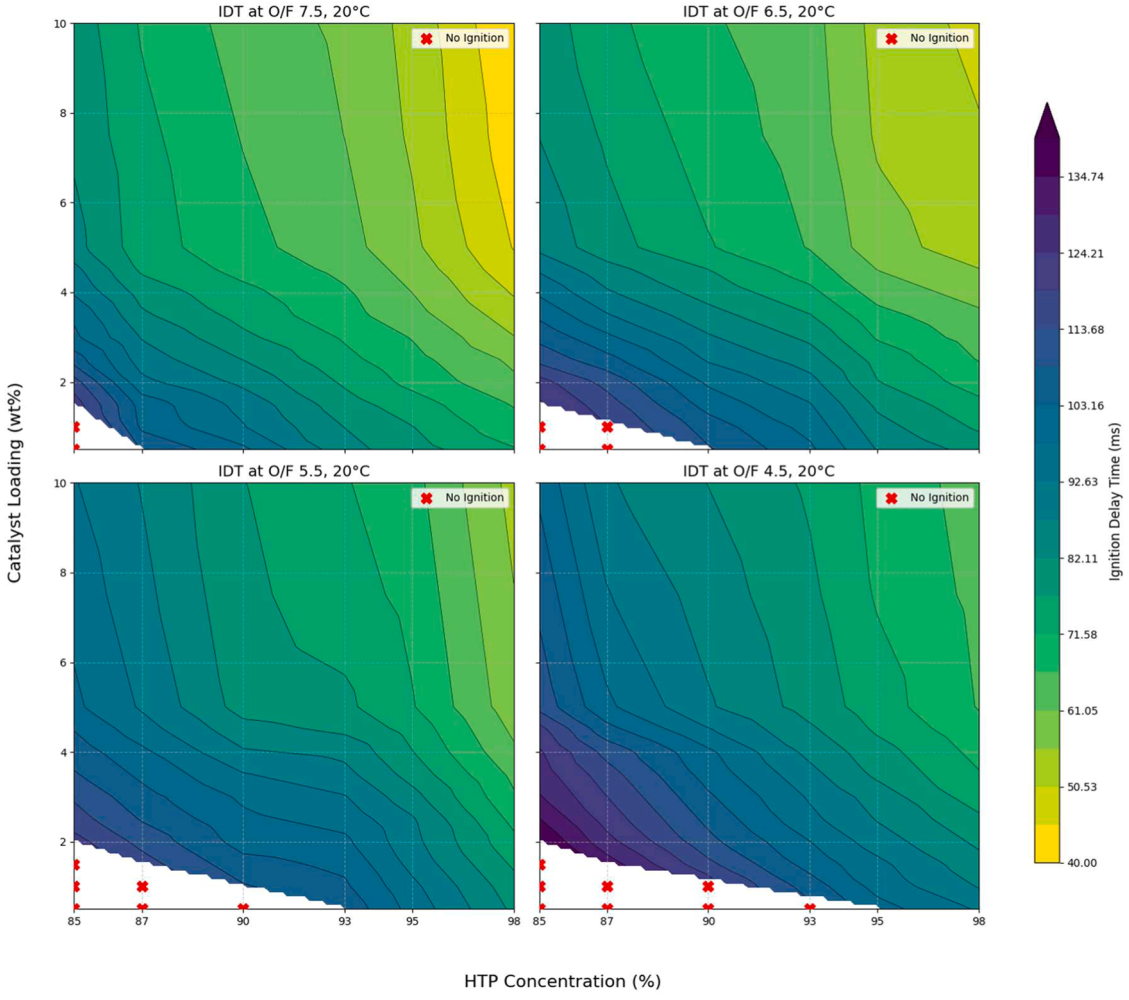

Fig. 1. Multi-panel contour plot illustrating the IDT as a function of HTP concentration and catalyst loading for various O/F ratios at 20°C. Red 'X' markers indicate conditions where no ignition was observed, clearly delineating the hypergolic envelope.

3.2. Impact of catalyst loading and HTP concentration on IDT

The data consistently show that increasing both catalyst weight percentage and HTP concentration leads to a reduction in IDTs, indicating enhanced reaction kinetics. This trend is observed across all O/F ratios and initial temperatures. Higher HTP concentrations provide a greater oxidizing potential, which increases the rate of oxygen and reactive radical generation (e.g., hydroxyl radicals, superoxide ions), driving the subsequent fuel oxidation more vigorously [21,22]. Similarly, higher catalyst loadings offer more active sites, accelerating the initial decomposition of HTP and thus shortening the overall ignition process. For example, at 20°C and O/F 7.5, increasing HTP concentration from 93% to 98% at a constant 5 wt% catalyst reduced the IDT from 63 ms to 45 ms. Similarly, at 98% HTP and O/F 7.5, increasing catalyst from 2.5 wt% to 5 wt% at 20°C reduced IDT from 60 ms to 45 ms. Furthermore, the experimental sweep at lower loadings (0.5–2.5 wt%) identified a critical ignition threshold. At O/F 7.5, reliable ignition was not observed below 1.5 wt%, indicating that a minimum catalyst density is required to sustain the initial exotherm against heat dissipation losses.

All reported IDTs represent mean values from a minimum of 5 replicate tests, with standard deviations presented in Fig. 2 and the Supplementary Information (Section S4.1). The relatively narrow dispersion of these measurements (indicated by the error bars) demonstrates high experimental repeatability, particularly at higher catalyst loadings where the chemical kinetic driving force dominates over physical mixing irregularities. This consistency confirms the reliability of the Mn(III)AA system for practical propulsion applications.

A notable observation is the presence of diminishing returns in IDT reduction with increasing catalyst loading, particularly evident beyond 5 wt%. The relationship between catalyst concentration and IDT exhibits a distinct non-linear behavior; while initial additions (0.5 to 5 wt%) result in a rapid exponential decay of ignition delay, further loading saturates the reaction surface, leading to a plateau. For example, as quantified in Table 1, for O/F 7.5 and 98% HTP at 20°C, increasing catalyst from 2.5% to 5.0% yielded a 25.0% reduction in IDT (from 60 ms to 45 ms). However, a further increase from 5.0% to 7.5% catalyst resulted in a 6.7% reduction (from 45 ms to 42 ms), and from 7.5% to 10.0% catalyst, the reduction was only 4.8% (from 42 ms to 40 ms). A similar trend is observed at 50°C. These trends are clearly depicted in Fig. 2.

This observed plateau can be rationalized through a scaling analysis of the competing timescales. The ignition process is governed by the local Damköhler number (Da), defined as the ratio of the physical mixing timescale (t_{mix}) to the chemical reaction timescale (t_{chem}):

$$Da = \frac{t_{mix}}{t_{chem}}$$

At low loadings, the system operates in a kinetically controlled regime ($Da < 1$), where the availability of catalytic active sites is the limiting factor; thus, increasing the concentration significantly reduces (t_{chem}) and the total IDT. However, as the loading increases beyond 5 wt %, the chemical reaction accelerates to the point where it outpaces the physical transport of the oxidizer to the fuel interface. The system effectively transitions into a mixing-limited regime ($Da > 1$). In this state, further reducing t_{chem} via additional catalyst yields diminishing returns, as the overall global rate is restricted by the hydrodynamic limit of droplet diffusion and mixing efficiency. This phenomenon is crucial for optimizing catalyst utilization, establishing 5 wt% as a practical upper limit to balance performance with fuel energy density. The full IDT dataset is available in the Supplementary Information (Section S4.1).

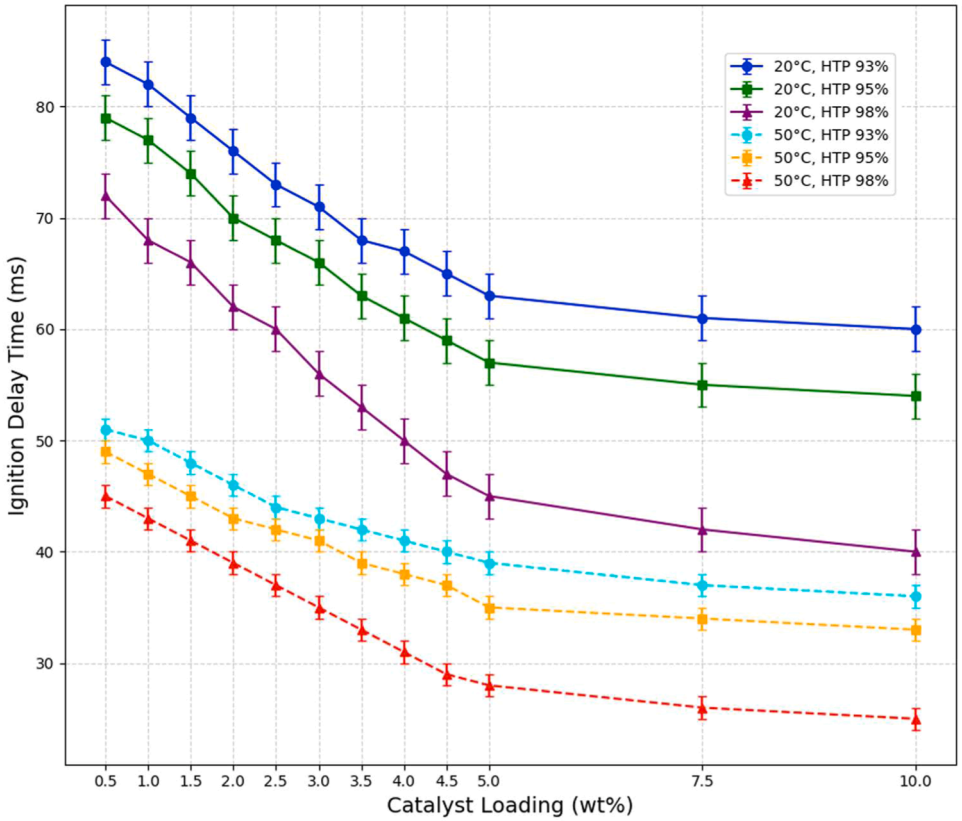

Fig. 2. IDT as a function of Catalyst Loading (wt%) for selected HTP concentrations (93%, 95%, 98%) at O/F 7.5 for both 20°C (solid lines) and 50°C (dashed lines). Error bars represent the standard deviation of IDT measurements. This plot visually emphasizes the diminishing returns in IDT reduction at higher catalyst loadings. Error bars represent the standard deviation calculated from n=5 replicates per condition.

Table 1
Percentage reduction in total IDT with increasing catalyst loading for O/F 7.5 and 98% HTP at 20°C and 50°C.

Catalyst Wt. % Increment			Initial Temperature (°C)	IDT (ms)		Absolute Reduction (ms)	Percentage Reduction (%)
Wt.%1		Wt.%2		Wt.%1	Wt.%2		
2.5 %	to	5.0 %	20	60	45	15	25.0
5.0 %	to	7.5 %	20	45	42	3	6.7
7.5 %	to	10.0 %	20	42	40	2	4.8
2.5 %	to	5.0 %	50	37	28	9	24.3
5.0 %	to	7.5 %	50	28	26	2	7.1
7.5 %	to	10.0 %	50	26	25	1	3.8

3.3. Effect of initial temperature on ignition performance

Elevating the initial temperature of the propellant system from 20°C to 50°C significantly enhances ignition performance across the entire parametric space. This temperature increase consistently leads to a substantial reduction in IDTs. For instance, at O/F 7.5, 10 wt% catalyst, and 98% HTP, the IDT drops from 40 ms at 20°C to 25 ms at 50°C, representing a 37.5% reduction. Across all conditions where ignition was observed at both temperatures, the average IDT reduction due to preheating to 50°C was approximately 30-40%. This pronounced effect of temperature highlights the strong temperature dependence of the overall hypergolic reaction. Beyond simply reducing delay times, the elevated temperature also plays a crucial role in expanding the hypergolic ignition envelope, enabling reliable ignition under conditions where it was previously absent at 20°C. For example, at O/F 4.5, 1.5 wt % catalyst, and 85% HTP, no ignition was observed at 20°C, but a reliable IDT of 101 ms was achieved at 50°C. Similarly, at O/F 5.5, 1 wt % catalyst, and 87% HTP, ignition was absent at 20°C but occurred at 85 ms at 50°C, as illustrated in Fig. 3.

These examples highlight the ability of preheating to overcome initial kinetic barriers, making marginal propellant compositions reliably hypergolic. This expanded operational window is a significant practical advantage for propulsion system design. The fundamental reason for this temperature effect lies in the Arrhenius relationship: higher temperatures increase the kinetic energy of molecules, leading to more frequent and energetic collisions. This accelerates both the catalytic decomposition of HTP and the subsequent chemical reactions with kerosene, thereby shortening all phases of the ignition process. This is particularly important for the initial HTP decomposition, which is highly exothermic and provides the necessary thermal feedback to drive subsequent reactions. Analysis of the phase deconvolution data reveals that the chemical delay is the most temperature-sensitive phase, exhibiting the most significant reduction in duration with elevated temperature, while the physical and HTP decomposition delays show comparatively less sensitivity. The full IDT dataset, including "no ignition" conditions, is available in the Supplementary Information (Section S4.1).

3.4. Kinetic analysis: apparent activation energy (E_a) and Pre-exponential factor (A)

The apparent activation energy (E_a) and pre-exponential factor (A) provide fundamental insights into the kinetic behavior of the Mn(III)AA catalyzed hypergolic ignition. Assuming the global reaction rate (k) is inversely proportional to the ignition delay time (τ), the temperature dependence is described by the Arrhenius equation:

$$k \propto \frac{1}{\tau} = A\exp\left(-\frac{E_a}{RT}\right)$$

By taking the natural logarithm, we obtain the linearized form used to extract the kinetic parameters:

$$\ln\left(\frac{1}{\tau}\right) = \ln(A) - \frac{E_a}{RT}$$

where R is the universal gas constant (8.314 J $mol^{-1}K^{-1}$) and T is the absolute temperature in Kelvin. It is important to acknowledge that the activation energy (E_a) and pre-exponential factor (A) derived here are apparent values calculated using a two-point Arrhenius method (20°C and 50°C). While a multi-point analysis would provide higher statistical robustness, the temperature range was strictly limited to 50°C to ensure

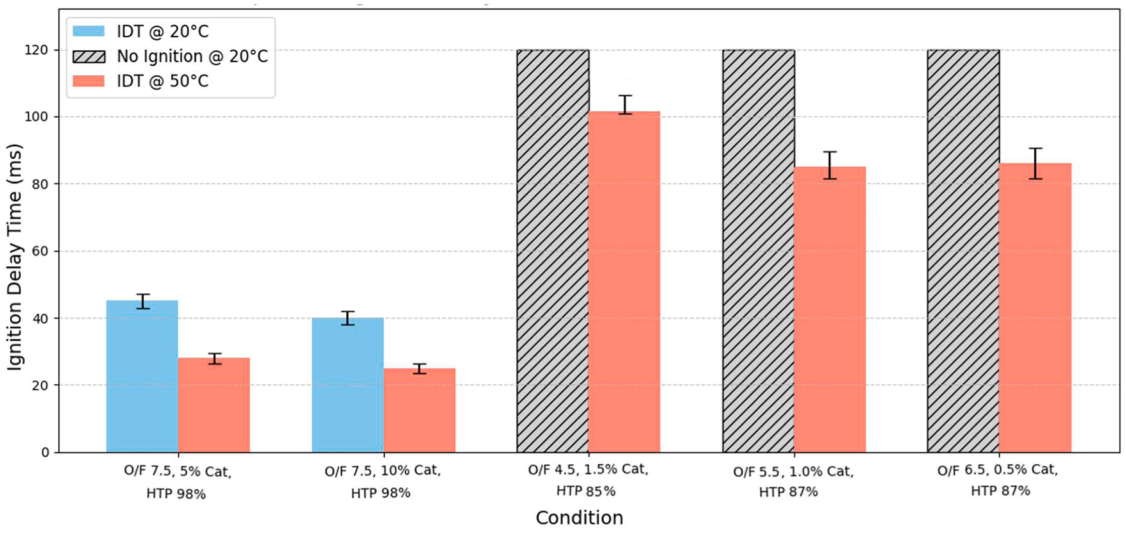

Fig. 3. Comparative IDT at 20°C versus 50°C for selected conditions at O/F 7.5. Light blue bars represent IDT at 20°C, and salmon bars represent IDT at 50°C. Hatched grey bars indicate conditions where no ignition was observed at 20°C, demonstrating the expansion of the ignition envelope at elevated temperatures. Error bars represent the standard deviation of IDT measurements.

laboratory safety; temperatures exceeding this threshold pose a significant risk of rapid, uncontrolled HTP decomposition before droplet impact in an open setup. Consequently, these parameters should be interpreted as global kinetic indicators for the coupled physical-chemical ignition process, rather than elementary reaction constants.

The calculated E_a values for Mn(III)AA across the reliable ignition conditions generally range from approximately 9 kJ/mol to 14 kJ/mol (detailed values are provided in Supplementary Information, Section S4.2). These relatively low activation energies are indicative of an efficient catalytic process, where Mn(III)AA significantly lowers the energy barrier for the overall ignition reaction compared to non-catalyzed or less effective systems. However, a specific mechanistic interpretation is warranted: in heterogeneous catalytic systems, activation energies in this lower range typically indicate that the overall reaction rate is partially governed by diffusion or mass-transfer limitations, which exhibit significantly weaker temperature dependence than intrinsic chemical kinetics. This suggests that the catalyst effectively lowers the chemical barrier to such an extent that physical mixing dynamics become the dominant weighting factor in the apparent system-level kinetics.

Analysis of the kinetic data reveals distinct sensitivity trends. The apparent activation energy (E_a) exhibits a strong dependence on the O/F ratio, decreasing from ~13 kJ/mol at O/F 7.5 to ~9 kJ/mol at O/F 4.5. This variation implies that the global energy barrier is modulated by the macroscopic stoichiometry and the associated physical mixing dynamics. In contrast, the pre-exponential factor (A) scales predominantly with catalyst loading, reflecting the increased frequency of active site collisions.

The pre-exponential factor (A), which reflects the frequency of effective molecular collisions and the number of active catalytic sites, ranges from approximately 311 s^{-1} to 4170 s^{-1} (detailed values in Supplementary Information, Section S4.2). Consistent with the observed IDT trends, A generally increases with higher HTP concentrations and catalyst loadings. This indicates that a greater concentration of reactive species and more available catalytic sites lead to a higher frequency of successful ignition events. The magnitude of A values, particularly at higher catalyst loadings and HTP concentrations, suggests a highly efficient pathway for the formation of reactive intermediates necessary for ignition.

Crucially, while the IDT is significantly influenced by temperature, the pre-exponential factor (A) itself shows minimal dependence on temperature, consistent with classical Arrhenius assumptions, within the tested range (20°C to 50°C), as evidenced by the nearly identical A values at both temperatures, as seen in Table 2 (detailed in Supplementary Information, Section S4.2). This implies that the pronounced reduction in IDTs observed at elevated temperatures (as illustrated in Fig. 3) is primarily driven by the exponential term ($e^{(-Ea\ /(R\cdot T))}$ within the Arrhenius equation, specifically the lowering of the activation energy barrier, rather than a significant change in the frequency of effective molecular collisions or the number of active catalytic sites.

Furthermore, the behavior of the A factor further supports the concept of diminishing returns with increasing catalyst loading. While A continues to increase as more catalyst is added, the rate of this increase slows down significantly, particularly beyond 5 wt%. This suggests that the system approaches a saturation point where additional catalyst no longer proportionally contributes to an increase in effective collisions or reactive sites. This could be due to the catalyst reaching its maximum surface area for interaction, where all available active sites are already engaged, or the rate of product removal from the active sites becoming a bottleneck. Alternatively, physical mixing limitations between the HTP decomposition products and the kerosene fuel could become dominant over chemical kinetics at higher catalyst concentrations, thus limiting further improvements in the overall reaction rate despite increased catalytic potential. This kinetic insight is vital for optimizing catalyst use, ensuring high performance without excessive material consumption. These trends are further illustrated in Fig. 4.

Table 2
Representative apparent activation energy (E_a) and Pre-exponential Factor (A) values for selected conditions at O/F 7.5 and O/F 6.5, showing general trends with HTP concentration and catalyst loading. (The full table of all calculated E_a and A values is available in the Supplementary Information (Section S4.2).

O/F	HTP Conc %	Cat Wt. %	E_a (kJ/mol)	A (s^{-1})
7.5	98	2.5	12.691	3043.37
		3.5	12.438	3105.44
		5.0	12.456	3684.15
	95	2.5	12.649	2639.77
		3.5	12.590	2780.59
		5.0	12.803	3354.58
	93	2.5	13.291	3199.23
		3.5	12.649	2639.77
		5.0	12.590	2780.59
6.5	98	2.5	10.645	1194.68
		3.5	10.857	1387.66
		5.0	10.893	1647.64
	95	2.5	11.175	1306.91
		3.5	11.429	1599.34
		5.0	11.101	1639.56
	93	2.5	11.910	1559.09
		3.5	12.407	2110.51
		5.0	11.866	1971.86

3.5. Post-ignition flame characteristics and mechanistic phases

The energy release and combustion efficiency of the Mn(III)AA catalyzed system are further characterized by the post-ignition flame temperatures and the deconvolution of the total IDT into its constituent phases.

Post-ignition flame temperatures, measured for O/F 6.5 and 7.5 at 93%, 95%, and 98% HTP concentrations (for catalyst loadings between 2.5% and 5%), ranged from approximately 940°C to 1240°C (detailed data in Supplementary Information, Section S4.3). Higher HTP concentrations and catalyst loadings generally correlated with higher flame temperatures, indicating more complete and energetic combustion. For instance, at O/F 7.5 and 98% HTP, flame temperatures increased from 1075°C at 2.5 wt% catalyst to 1240°C at 5.0 wt% catalyst. These high flame temperatures confirm the robust energy release from the Mn(III)AA catalyzed HTP/kerosene system, making it highly suitable for propulsion applications. Visual observations of the ignition and flame development are presented in Fig. 5.

High-speed camera footage provided crucial qualitative validation of the quantitative IDT data and mechanistic insights. At initial propellant contact, all conditions appeared identical, with no immediate visible reaction, which aligns with the inherent latency of hypergolic ignition. As the reaction progressed, elevated temperatures and higher catalyst loadings significantly accelerated the onset of visible pre-ignition activity, such as fume or gas evolution. This visual cue directly corresponded to the shortening of the HTP decomposition and physical IDT phases, consistent with faster thermal breakdown of HTP at 50°C (where decomposition started approximately 20-30% faster across all HTP concentrations). The "first light" (chemical ignition) consistently occurred earlier at 50°C and higher catalyst weight percentages; conversely, 20°C videos at comparable timestamps showed no visible flame, reflecting their longer total IDTs. Following chemical ignition, the flame grew faster and appeared more vigorous at higher temperatures and catalyst loadings. This rapid early flame development aligns with the higher post-ignition flame temperatures (e.g., >1100°C at 50°C, particularly at 5 wt% catalyst and 98% HTP). Flame stabilization was also achieved more rapidly with increased catalyst loading and elevated temperatures, visually manifesting as a steady, luminous flame formation within approximately 40 ms at 50°C compared to around 60 ms at 20°C. These visual observations provide strong qualitative confirmation of the quantitative data, including faster decomposition and chemical ignition stages, higher flame temperatures, and overall lower IDTs,

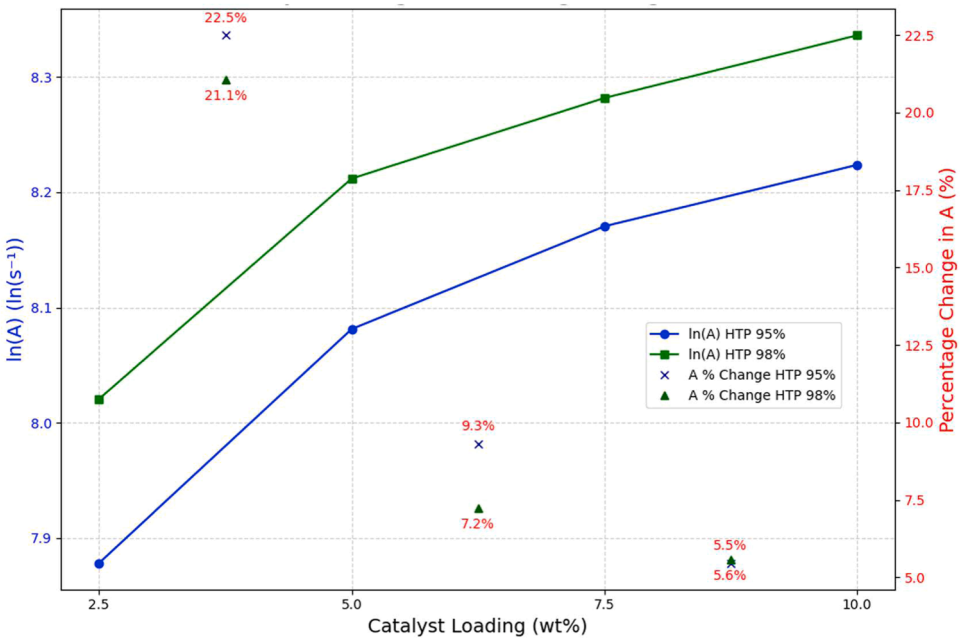

Fig. 4. Natural logarithm of the Pre-exponential Factor (ln(*A*)) as a function of Catalyst Loading (wt%) for HTP 95% (blue line) and HTP 98% (green line) at O/F 7.5 (*A* values derived from 20°C data). The 'x' and 'Δ' symbols, with accompanying numerical labels, represent the percentage change in *A* between consecutive catalyst loading increments, illustrating the diminishing returns in the rate of increase of *A*.

further supporting the diminishing returns observed at higher catalyst concentrations.

Analysis of the multi-phase ignition process provides deeper insight into the role of Mn(III)AA, illustrated in Fig. 6. The total IDT was segmented into HTP Decomposition Delay, Physical Delay, and Chemical Delay (details in Supplementary Information, Section S4.4). The data show that the chemical delay is often the most significantly impacted phase by the catalyst, indicating Mn(III)AA's primary role in accelerating the chemical reactions between the HTP decomposition products and kerosene fuel.

While the physical delay (related to mixing and vaporization) and HTP decomposition delay also contribute to the total IDT, their relative contributions might vary less significantly with catalyst loading compared to the chemical phase, especially at optimal conditions. This suggests that while Mn(III)AA effectively drives the chemical kinetics, physical processes can become rate-limiting, particularly at lower catalyst loadings or less ideal mixing conditions.

3.6. *Implications for pressurized systems and green propulsion*

The experimental results, obtained from open-air drop tests at ambient pressure, provide a strong foundation for understanding the performance of Mn(III)AA catalyzed hypergolic systems. It is crucial to consider that in practical propulsion systems, combustion occurs under pressurized conditions. Based on established literature trends for similar propellant systems, IDTs are expected to further reduce by approximately 20-30% in pressurized environments [12,20]. This projection suggests that the Mn(III)AA catalyzed HTP/kerosene combination could achieve IDTs in the low tens of milliseconds or even single-digit milliseconds, which would surpass or significantly compete with the performance of many conventional and other propellants currently used in propulsion applications.

However, the extrapolation of the 'diminishing returns' trend observed at high catalyst loadings warrants specific consideration. High chamber pressures significantly increase the chemical reaction rate ($Rate \propto P^n$), potentially shrinking the chemical delay phase to a negligible duration relative to physical processes. Consequently, the total ignition delay becomes increasingly dominated by atomization, vaporization, and mixing dynamics. This suggests that the plateauing effect of catalyst loading observed here (beyond 5 wt%) may become even more pronounced in pressurized systems, as the system shifts rapidly towards a mixing-limited regime where additional chemical catalyst provides minimal benefit. Therefore, in operational engines, injector design, specifically atomization efficiency, will likely govern performance more critically than higher catalyst concentrations.

Beyond chamber pressure, practical implementation must also contend with extreme environmental conditions. Specifically, ignition in low-pressure atmospheres (high-altitude or vacuum conditions) introduces the risk of flash vaporization. This phenomenon can induce rapid evaporative cooling, significantly lowering the droplet surface temperature and prolonging the physical delay phase. Furthermore, thermal management remains a critical challenge. High thermal conductivity within the injector assembly or the propellant bulk can rapidly dissipate the exothermic heat generated at the contact interface. If this heat loss exceeds the rate of chemical heat release, the reaction kernel may be quenched before a self-sustaining flame is established. Future system-level testing must therefore optimize injector geometry to minimize conductive heat loss during the critical ignition transient.

The high performance, coupled with the inherent advantages of HTP (non-toxicity, benign decomposition products) and the efficiency of Mn(III)AA (effective at low catalyst loadings), positions this system as a highly viable and sustainable alternative for future space propulsion. The elimination of complex ignition systems and conventional catalyst beds due to the intrinsic hypergolicity further contributes to simplified engine designs, reduced manufacturing and operational costs, and enhanced safety during handling and launch operations. This research therefore offers a significant step towards developing more efficient, reliable, and environmentally responsible propulsion technologies, aligning with the growing demand for sustainable space exploration.

4. Conclusions

In conclusion, this study establishes Manganese(III) acetylacetonate (Mn(III)AA) as a highly potent catalyst for enabling hypergolic ignition in non-polar aviation kerosene (Jet A-1) with 98% HTP. The key scientific and practical findings are summarized as follows:

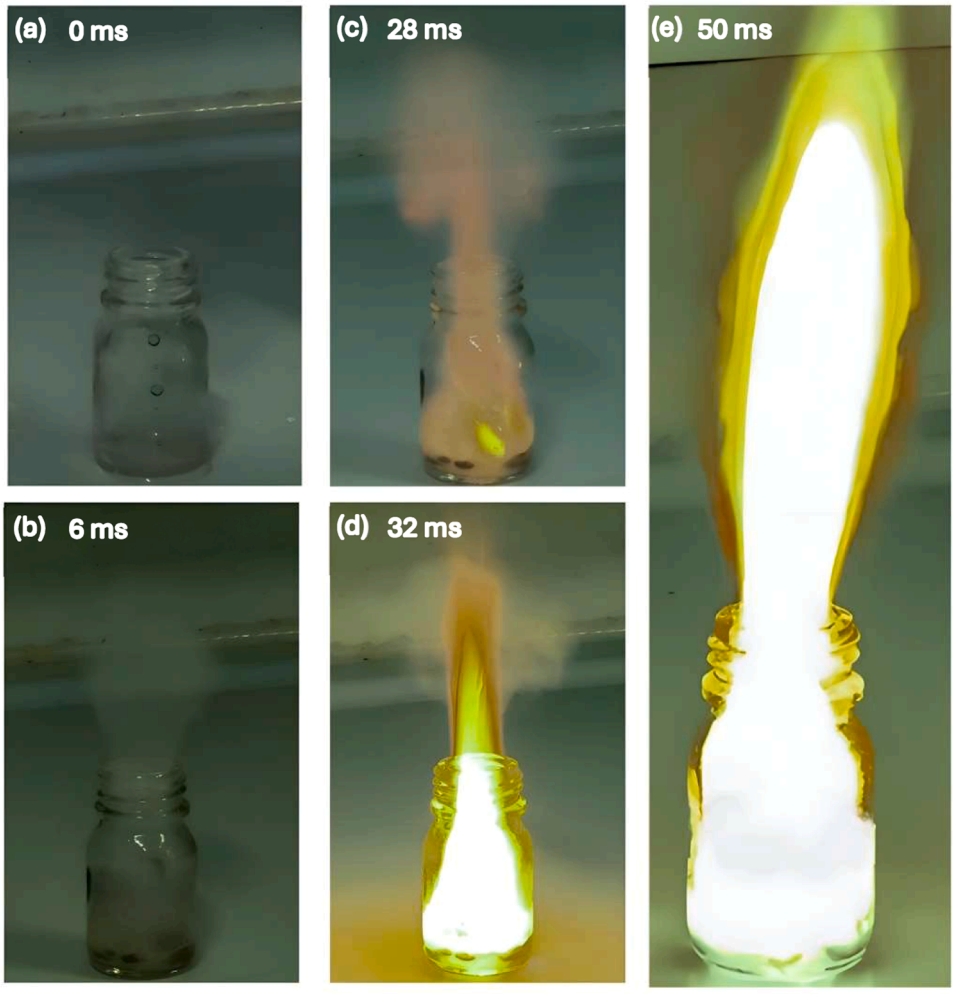

Fig. 5. A visual sequence of high-speed camera images showing the ignition and flame development for O/F 7.5, 98% HTP, 5 wt% catalyst at 50°C. The sequence highlights (a) initial droplet contact, (b) HTP decomposition, (c) first light (chemical ignition), (d) early flame growth, and (e) eventual flame stabilization, demonstrating the vigorous and stable combustion process.

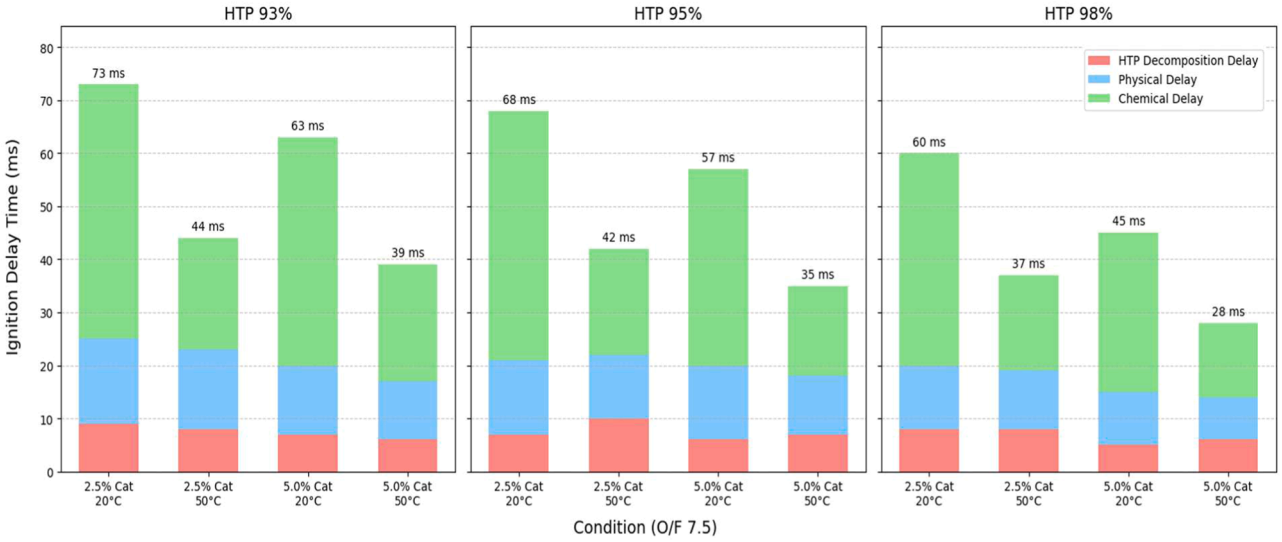

Fig. 6. Stacked bar charts illustrating the relative contribution of HTP Decomposition Delay, Physical Delay, and Chemical Delay to the total IDT for O/F 7.5 at HTP concentrations of 93%, 95%, and 98%. Each subplot compares 2.5% and 5.0% catalyst loadings at both 20°C and 50°C.

1. Catalytic Efficiency: The system achieved a minimum Ignition Delay Time (IDT) of 25 ms at 50°C, a result that significantly outperforms non-catalyzed hydrocarbon systems (>100 ms) and rivals complex ethanol-gel propellants [12].
2. Optimal Loading Threshold: A distinct non-linear kinetic behavior was identified, where catalyst efficiency saturates beyond 5 wt%. This observation defines a critical design limit, confirming that once the chemical barrier is sufficiently lowered, the system becomes governed by physical mixing rates ($Da > 1$). Thus, further performance gains in operational engines should be sought through injector atomization improvements rather than increased chemical loading.
3. Mechanism of Action: Kinetic analysis revealed that Mn(III)AA significantly lowers the activation energy ($E_a \sim$ 9-12 kJ mol^{-1}), effectively accelerating the chemical delay phase to the point where physical mixing processes become the rate-limiting step.

From a propulsion system integration perspective, the trade-off between kinetic performance and rheological practicality is critical. While catalyst loadings up to 10 wt% demonstrated the shortest ignition delays, such high solid-loading slurries introduce risks regarding long-term storage stability (sedimentation) and injector compatibility (clogging or altered atomization patterns due to increased viscosity). Consequently, the 5 wt% loading is identified as the optimal operational point, offering a robust balance where reliable hypergolic ignition is achieved without incurring the severe penalty of poor propellant homogeneity or feed-system hydraulic losses.

It is important to acknowledge the limitations of this experimental approach. The results presented here were obtained under ambient pressure conditions. While valuable for screening, the absolute IDT values may differ in pressurized combustion chambers due to enhanced reaction rates and altered atomization regimes. Therefore, the high-pressure performance suggested by literature trends remains a theoretical projection requiring direct experimental validation in future chamber testing. Furthermore, the kinetic parameters reported are apparent values derived from a two-point temperature range, serving as global performance indicators rather than elementary reaction constants.

Future research should prioritize validating these findings in pressurized combustion chambers to quantify the influence of chamber pressure on the catalyst saturation threshold. Additionally, investigations into the long-term storage stability of Mn(III)AA in kerosene and cold-flow atomization studies are recommended to optimize injector geometries for this specific propellant combination. Finally, ignition testing under vacuum conditions is necessary to assess performance risks related to flash vaporization in upper-stage applications.

Nomenclature

Abbreviation / Symbol	*Description*
HTP	*High Test Peroxide*
Mn(III)AA	*Manganese(III) acetylacetonate*
IDT	*Ignition Delay Time (ms)*
O/F	*Oxidizer-to-Fuel Ratio*
E_a	*Activation Energy (kJ mol^{-1})*
A	*Pre-exponential Factor (s^{-1})*
R	*Universal Gas Constant (8.314 J mol^{-1} K^{-1})*
T	*Temperature (K or °C)*
ROI	*Region of Interest*
FPS	*Frames Per Second*

CRediT authorship contribution statement

Prakhar Jindal: Writing – original draft, Visualization, Validation, Resources, Methodology, Investigation, Funding acquisition, Formal analysis, Data curation, Conceptualization. **Jyoti Botchu:** Writing – review & editing, Supervision, Project administration, Funding acquisition.

Declaration of competing interest

The authors declare that they have no known competing financial interests or personal relationships that could have appeared to influence the work reported in this paper.

Acknowledgements

This paper is based upon the work supported by Horizon Europe's research and innovation programme under the Marie Sklodowska-Curie grant agreement No. 101107214. The authors acknowledge the extensive support from the Space System Engineering section of the Faculty of Aerospace Engineering, Delft University of Technology, Netherlands.

Supplementary materials

Supplementary material associated with this article can be found, in the online version, at doi:10.1016/j.ast.2026.112056.

Data availability

Data will be made available on request.

References

[1] R.L. Sackheim, RK. Masse, Green propulsion advancement: challenging the maturity of monopropellant hydrazine, J. Propuls. Power. 30 (2014) 265–276, https://doi.org/10.2514/1.B35086. ISSUE:ISSUE:10.2514/JPP.2014.30.ISSUE-2; PAGE:STRING:ARTICLE/CHAPTER.
[2] A.S. Gohardani, J. Stanojev, A. Demairé, K. Anflo, M. Persson, N. Wingborg, et al., Green space propulsion: opportunities and prospects, Prog. Aerosp. Sci. 71 (2014) 128–149, https://doi.org/10.1016/J.PAEROSCI.2014.08.001.
[3] E.S. Williams, J. Panko, DJ. Paustenbach, The European Union's REACH regulation: a review of its history and requirements the EU REACH regulation: a review E. S. Williams et al, Crit. Rev. Toxicol. 39 (2009) 553–575, https://doi.org/10.1080/10408440903036056;SUBPAGE:STRING:ACCESS.
[4] Y. Ju, C. Song, BJ. Lee, Guidelines for the safe handling of hypergolic propellants in development of space propulsion systems, J. Propuls. Energy 4 (2024) 42–57, https://doi.org/10.6108/JPNE.2024.4.1.042.
[5] A.E.S. Nosseir, A. Cervone, A. Pasini, Review of state-of-the-art green monopropellants: for propulsion systems analysts and designers, Aerospace 8 (2021) 20, https://doi.org/10.3390/AEROSPACE8010020. Vol 8, Page 20 2021.
[6] Scharlemann C. Green propellants: global assessment of suitability and applicability. 2020, n.d.
[7] R. Amrousse, Q-L. Yan, Recent Advancements in Green Propulsion, Springer, 2024.
[8] G. Rarata, K. Rokicka, P. Surmacz, Hydrogen peroxide as a high energy compound optimal for propulsive applications, Cent. Eur. J. Energ. Mater. 13 (2016) 778–790.
[9] Lin W-C, Young G, Schetz JA, Massa L, Liu G. Experimental and theoretical study of hypergolic solid fuel ignition and combustion with hydrogen peroxide 2025.
[10] U. Swami, N. Kumbhakarna, A. Chowdhury, Green hypergolic ionic liquids: future rocket propellants, J. Ion. Liq. 2 (2022) 100039, https://doi.org/10.1016/J.JIL.2022.100039.
[11] W. Florczuk, G. Rarata, Performance evaluation of the hypergolic green propellants based on the HTP for a future next-generation space crafts, in: 53rd AIAA/SAE/ASEE Joint Propulsion Conference, 2017, https://doi.org/10.2514/6.2017-4849.
[12] B.V.S. Jyoti, M.S. Naseem, SW. Baek, Hypergolicity and ignition delay study of pure and energized ethanol gel fuel with hydrogen peroxide, Combust. Flame 176 (2017) 318–325, https://doi.org/10.1016/J.COMBUSTFLAME.2016.11.018.
[13] X. Zhao, J. Wang, Y. Jin, K. Wang, Q. Zhang, Energetic complexes as promoters for the green hypergolic bipropellant of EIL-H2O2 combinations, FirePhysChem 2 (2022) 185–190, https://doi.org/10.1016/J.FPC.2021.11.006.
[14] S. Nath, I. Laso, L. Mallick, Z. Sobe, S. Koffler, B. Blumer-Ganon, et al., Comprehensive ignition characterization of a non-toxic hypergolic hybrid rocket propellant, Proc. Combust. Inst. 39 (2023) 3361–3370, https://doi.org/10.1016/J.PROCI.2022.07.118.
[15] W. Florczuk, G. Rarata, Assessment of various fuel additives for reliable hypergolic ignition with 98%+ HTP. 66th International Astronautical Congress, in: International Astronautical Federation Jerusalem, 2015.
[16] Ł Boruc, ŁJ Kapusta, J. Kindracki, Selection of the method for determination of ignition delay of hypergolic propellants, Combust. Engines 199 (2024) 104–111.
[17] Z. Qiao, Y. Li, Q. Miao, H. Ma, L. Xu, R. Li, Experimental investigation of obstruction effects on C3H8/H2 hybrid fuel explosion dynamics in semiconfined pipelines, ACS. Omega 10 (2025) 35954–35964, https://doi.org/10.1021/ACSOMEGA.5C03366.

[18] J. Huang, Y. Li, Z. Zhou, M. Xiang, Study on the impact of the atomized water droplet size on the performance of magnesium-based water ramjet engine, Appl. Therm. Eng. 279 (2025) 127849, https://doi.org/10.1016/J.APPLTHERMALENG.2025.127849.

[19] D.A. Castaneda, B. Natan, Hypergolic ignition of hydrogen peroxide with various solid fuels, Fuel 316 (2022) 123432, https://doi.org/10.1016/J.FUEL.2022.123432.

[20] ŁJ Kapusta, Ł Boruc, J. Kindracki, Pressure and temperature effect on hypergolic ignition delay of triglyme-based fuel with hydrogen peroxide, Fuel 287 (2021) 119370, https://doi.org/10.1016/J.FUEL.2020.119370.

[21] Y. Li, L. Li, Z.X. Chen, J. Zhang, L. Gong, Y.X. Wang, et al., Carbonate-activated hydrogen peroxide oxidation process for azo dye decolorization: process, kinetics, and mechanisms, Chemosphere 192 (2018) 372–378, https://doi.org/10.1016/J.CHEMOSPHERE.2017.10.126.

[22] C. Tizaoui, N. Karodia, M. Aburowais, Kinetic study of the manganese-based catalytic hydrogen peroxide oxidation of a persistent azo-dye, J. Chem. Technol. Biotechnol. 85 (2010) 234–242, https://doi.org/10.1002/JCTB.2293. REQUESTEDJOURNAL:JOURNAL:10974660;JOURNAL:JOURNAL:10974660; WGROUP:STRING:PUBLICATION.